AALBORG UNIVERSITY

Thermal Loss Becomes an Issue for Tunable Narrow-band Antennas in Fourth Generation Handsets

Barrio, Samantha Caporal Del; Morris, Art; Pedersen, Gert Frølund

Thermal Loss Becomes an Issue for Narrow-band Tunable Antennas in 4G Handsets

Samantha Caporal Del Barrio, Art Morris and Gert F. Pedersen

Abstract

Antenna tuning is a very promising technique to cope with the expansion of the mobile communication frequency spectrum. Tunable antennas can address a wide range of operating frequencies, while being highly integrated. In particular, high-Q antennas (also named narrow-band antennas) are very compact, thus are good candidates to be embedded on 4G handsets. This paper focuses on *high-Q* tunable antennas and contributes with a characterization of their loss mechanism, which is a major parameter in link-budget calculations. The paper shows through an example, that the tuner loss is not sufficient to explain the total loss of tunable antennas. It is found that, thermal loss - due to the metal conductivity of the antenna itself - plays a major role in the loss mechanism of narrow-band tunable antennas. The investigated high-Q PIFA designs exhibit a significant thermal loss; at 1400 MHz nearly 2 dB are lost solely due to the copper conductivity. Thermal loss poses a limitation to achievable performance of tunable antennas and to antenna miniaturization.

Index terms—4G mobile communication, Antenna measurements, Reconfigurable architectures, Tunable circuits and devices.

1 Introduction

The user demand for ever increasing data rates has driven the development of the 4th Generation (4G) of mobile communication standards. This new generation poses major challenges on the requirements for handset antennas. On the one hand the number of bands to support has increased to 26 bands ranging from 700 MHz to 2.69 GHz [1], on the other hand the volume dedicated to the antenna has shrunk in order to fit several antennas, add more cameras and enlarge the battery, among others. However, fundamental limitations relate the antenna efficiency, size and bandwidth at a given frequency [2]. Indeed, passive designs need to increase the antenna volume, in order to simultaneously increase its bandwidth and maintain its efficiency. Oppositely, Frequency-Reconfigurable Antennas (FRA) can operate in a wide range of frequencies, without modifying their geometry. Integrated active components modify the antenna reactance, consequently shifting the resonance frequency. Frequency-reconfigurability can be achieved with the integration of switches, variable capacitors, phase shifters or tunable substrates in the antenna structure. Most commonly, FRA's use PIN diodes [3,4], varactor diodes [5,6], Micro-Electro-Mechanical Systems (MEMS) switches [7,8], or MEMS tunable capacitors [9–11]. As detailed in [12], switched capacitors - e.g. field effect transistors (FET) - lead to an intrinsically low breakdown voltage and power handling, thus limiting its application for 4G handsets [13]. PIN diodes can handle more power; though, they exhibit a higher insertion loss, a smaller tuning range, and a higher power consumption [14]. Tunable substrates are an alternative to switches, revealing a higher Q. However, they use barium strontium titanate (BST), which causes issues with linearity. MEMS tunable capacitors are the most promising tuning technology. They exhibit beams that are actuated by electrostatic forces. Each beam can have two states, down (i.e., on) or up (i.e., off). When the beam is down, only dielectric separates it from the metal trace below it. When the beam is up, an additional air gap separates the beam from the metal trace [13]. Because the RF path is a metal trace, MEMS capacitors offer significantly higher performance, than previous solutions. MEMS tunable solutions are state-of-the-art in terms of insertion loss,
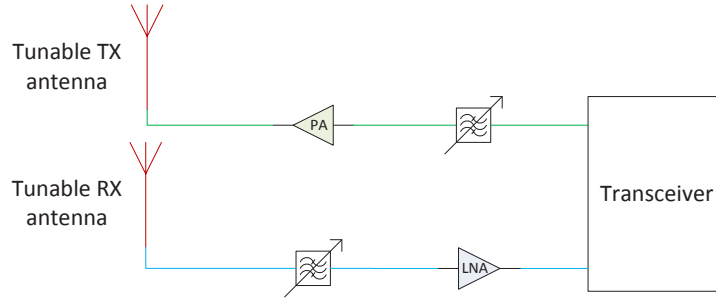
Figure 1: A front-end architecture using narrow-band FRA's [9].

voltage handling, linearity and power consumption, hence this paper uses MEMS tunable capacitors. With frequency-reconfigurability, the antenna element can be both small and able to cover a large bandwidth. The element is small because of its high natural resonance frequency and its narrow instantaneous bandwidth. The geometry is unchanged as the antenna is operating at lower frequencies. FRA's have a huge potential for the implementation of current and future mobile communications standards on a small platform.

The properties of FRA's are fully exploited when one considers a system, where the antenna only needs to cover a channel, as opposed to a full band. In the Long Term Evolution (LTE) standard [1], channel bandwidths vary from 1.4 MHz to 20 MHz. The antenna − only needing to cover a narrow bandwidth − exhibits a high Q and can be designed with a very low profile. Additionally, limiting the antenna instantaneous bandwidth to channel bandwidths implies having a novel architecture that supports separate antennas for Transmitting (Tx) and Receiving (Rx) signals, i.e. the number of antennas must be doubled. Such an architecture was first conceptualized in [15] and investigated in [9, 10, 16, 17] according to the patent [18]. The major strength of such architecture is to avoid the use of duplex filters, hence avoiding component duplication, which will reduce space, cost and battery consumption. Fig. 1 represents the front-end of such a system for a mobile phone. Removing the duplex filter from the front-end architecture also requires to get the necessary Tx-Rx isolation from the tunable antennas and from the tunable filters. One of the main challenges of the proposed architecture is to obtain the required antenna isolation on a small platform, e.g. mobile phones. Previous work has mainly been focusing on that aspect [16, 17, 19]. This work focuses on another critical aspect of the proposed architecture: *the efficiency of reconfigurable high-Q antennas.* These low-profile antennas are very attractive for today's phone market, given their small volume. However, they exhibit a large Q, which results in high fields confined around the antenna structure and in the tuner. FRA's have a large Q, that increases considerably as their resonance frequency is tuned further away from its initial value. Along with this increase in Q comes a dramatic radiation efficiency drop, e.g. 3 dB were reported in [20] for 100 MHz tuning.

This paper aims at identifying and characterizing the sources of loss in narrow-band reconfigurable antennas. The novelty of this study lies in investigating high-Q antennas, that are frequency-reconfigurable with MEMS tunable capacitors and for mobile phone application. The study focuses on the low-bands of the 4G spectrum, as they are the toughest to address with small antennas, given the large wavelengths. Specifically, the cause of efficiency degradation throughout tuning is investigated. Section II investigates the loss due to the tuner while Section III addresses the loss due to the conductivity of the metal. Finally, Section IV discloses the conclusions on the loss mechanism of narrow-band FRA's for handsets.

2 Tuner Loss

The tuner specifications investigated in the following are taken from a commercially available MEMS tunable capacitor. It is able to deliver a variable capacitance ranging from 1 pF to 8 pF, with steps of 125 fF [21].

2.1 Simulations parameters

The following simulations aim at comparing the impact of the tuner loss on the efficiency of a high-Q and a low-Q FRA. Comparisons are made for several positions of the capacitor (C_{pos}) and tuned frequencies of the antennas. More precisely, this section investigates the impact of the tuner insertion loss on the antenna, depending on the antenna Q. The loss of the tuner is due to its Equivalent Series Resistance (ESR), which
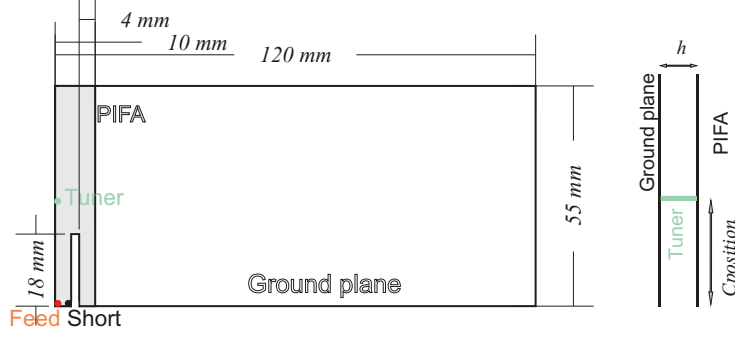
Figure 2: Antenna design (A1: h=8 mm, A2: h=2 mm) [12].

Table 1: Capacitance and ESR for the low-Q antenna

	C_{pos}=5	C_{pos}=10	C_{pos}=20	C_{pos}=30
	pF/Ω	pF/Ω	pF/Ω	pF/Ω
900 MHz	1.125/0.405	0.500/0.405	0.125/1.369	0.125/1.369
850 MHz	1.750/0.179	0.875/0.249	0.375/0.478	0.250/1.071
800 MHz	2.250/0.125	1.375/0.182	0.625/0.279	0.500/0.438
750 MHz	2.875/0.119	1.875/0.150	1.000/0.198	0.750/0.403
700 MHz	3.500/0.114	2.375/0.126	1.375/0.203	1.000/0.202

Table 2: Capacitance and ESR for the high-Q antenna

	C_{pos}=5	C_{pos}=10	C_{pos}=20	C_{pos}=30
	pF/Ω	pF/Ω	pF/Ω	pF/Ω
900 MHz	3.125/0.119	1.500/0.106	0.625/0.285	0.375/0.457
850 MHz	5.125/0.090	2.625/0.127	1.125/0.105	0.875/0.385
800 MHz	6.875/0.101	3.875/0.125	1.750/0.148	1.250/0.195
750 MHz	8.625/0.081	5.125/0.089	2.500/0.127	1.875/0.150
700 MHz	10.500/0.093	6.375/0.097	3.375/0.114	2.500/0.127

is intrinsic to its manufacturing. In order to quantify the tuner loss, its contribution to the total efficiency is isolated, i.e. the antenna element and the Ground Plane (GP) are simulated as Perfect Electric Conductor (PEC). The simulations are conducted with the transient solver of CST [22]. Both high-Q and low-Q antennas are designed for 960 MHz, and are tuned until 700 MHz. In order to fairly compare the impact of the ESR loss in the different tuning stages and locations, identical power needs to be transferred between the source and the antenna port. Consequently, the tuned antennas must be perfectly matched to the source impedance. In order to isolate the contribution of the ESR of the tuning capacitor, the matching to the source impedance is done with lossless components. All the following results are normalized to 1 W input power.

The low-Q and the high-Q PIFA designs only differ by the height of the antenna element over the GP. The design and dimensions of the antennas are presented in Fig. 2. The low-Q antenna (A1) is placed 8 mm over the GP whereas the high-Q antenna (A2) is placed only 2 mm over the GP. The GP has the dimensions 120 x 55 mm^2 in order to fit modern phone designs. The tuning capacitor is placed between the antenna element and the GP connecting the two plates. C_{pos} represents the position of the tuning capacitor in mm from the source position.

2.2 Simulation results

Due to the inaccessibility of the exact data on the ESR values of this tuning capacitor for all its settings, the ESR values have been taken from the low-ESR GJM 15 data bank of 0402 Murata fixed components [23]. These fixed capacitors have been chosen because they exhibit similar Q at maximum capacitance of the MEMS at 1 GHz. The data for the tuning capacitor simulated on the low-Q antenna is shown in Table. 1 and the data for the tuning capacitor simulated on the high-Q antenna is shown in Table. 2.
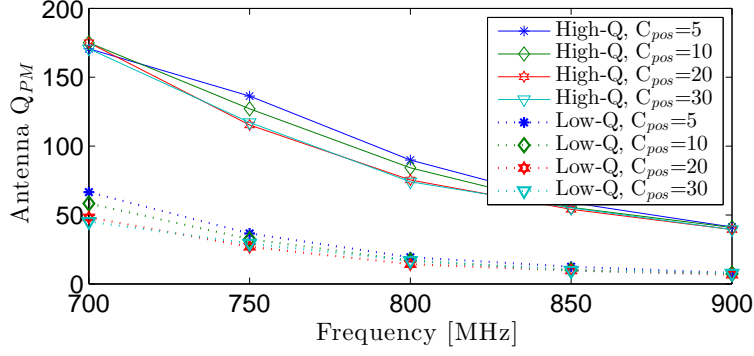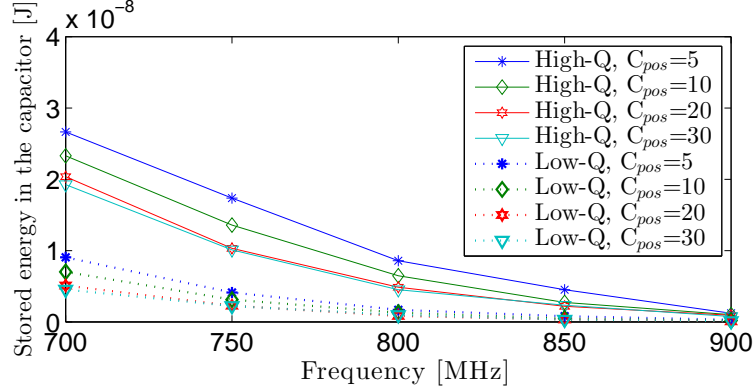
Figure 3: Q of A1 and A2 throughout tuning.

Figure 4: Energy stored in the tuning capacitor throughout tuning.

2.2.1 Antenna Q

The Quality factor (Q) of the antenna is a measure of the stored energy in the radiating structure [24]. The Perfectly Matched Q (Q_{PM}) is calculated according to [24] and further detailed in Section III. The Q of the antennas at their natural resonance are 5 and 32, for the low-Q and the high-Q antennas respectively. The low height of A2 results in a Q that is 6 times larger and the bandwidths at -6 dB (BW_{-6dB}) are 222 MHz and 35 MHz, for the low-Q and the high-Q antennas respectively. The low height of A2 results in an increase in Q_{PM} of 540 %.

Fig. 3 shows the increase in Q_{PM} of the high-Q and the low-Q FRA as the frequency is tuned further away from the natural resonance. The increment in Q_{PM} is clearly steeper for the high-Q antenna, and its value at 700 MHz is more than three times larger than for the low-Q antenna. One can notice that the Q_{PM} is not constant across frequency, nor is the increasing factor across frequency. These factors are also different from the low-Q to the high-Q antennas. Additionally the position of the tuning capacitor does not seem to have a large effect on the Q_{PM}. The Q_{PM} value seems to be driven by the frequency of operation, compared to the natural resonance frequency of the design.

2.2.2 Efficiency

The reactive energy in the capacitor is a measure of the energy that is stored in the capacitor in order to force the antenna resonance into a different frequency. This energy is not radiated by the antenna and is independent of the ESR. It is plotted in Fig. 4 for the high-Q and the low-Q antennas. It can be observed that the energy that is stored in the capacitor in order to tune the high-Q antenna is considerably higher than the energy that is needed to tune the low-Q antenna. This phenomenon happens because the capacitance values that are required to tune the high-Q antenna are considerably higher than the values required for the low-Q antenna, given its narrow bandwdith.

The dissipated power in the ESR is plotted in Fig. 5. The high fields of the high-Q antenna impact significantly the tuner loss, compared to the low-Q antenna case. Additionally, the placement of the tuner
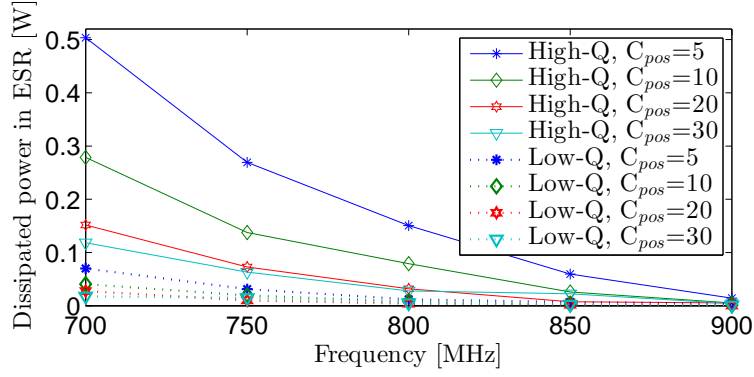
4

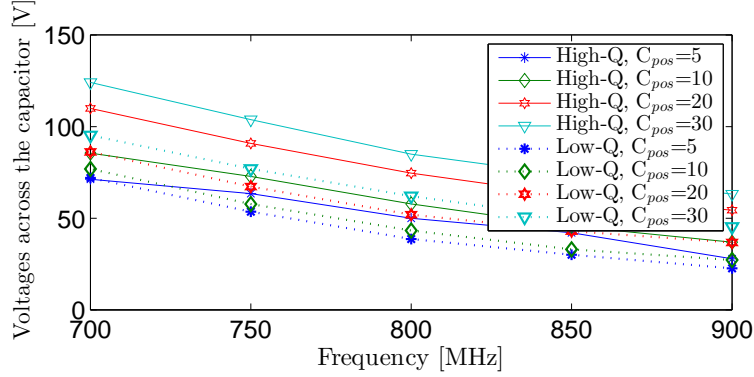Figure 5: Dissipated power due to the ESR of the tuner.

Figure 6: Voltages across the tuner.

affects the capacitance needed for tuning, the currents to the capacitor, its stored energy and therefore the power dissipated by the ESR. The loss due to the ESR of the capacitor is proportional to the square of the currents delivered to it. In the case where the capacitor is located the closest to the source on the high-Q antenna, the ESR is responsible for up to 3 dB of loss. From an efficiency point of view, narrow-band antennas should have the tuner placed as far as possible from the source location. The furthest possible location of the tuner is limited by its voltage breakdown value. Voltages across the tuning capacitor are shown in Fig. 6.

2.2.3 Metal conductivity

The impact of varying the conductivity of the antenna and the GP on the power dissipated by the varactor is investigated. The results are shown for the high-Q antenna, as it exhibits the highest loss, and for C_{pos}=10mm. Several materials are investigated. Their conductivity (σ) and wavelength (λ) are summarized in Table 3. Results are shown in Fig. 7. Negligible differences are observed between the copper and the silver simulations, as conductivity values are very similar. Moreover, for early stages of tuning, the power dissipated by the tuning capacitor does not vary depending on the conductivity of the metal. However, as the antenna is tuned further away from its original resonance frequency and as its Q increases, the power dissipated by the tuner is dependent on the metal conductivity of the antenna. More specifically, the power dissipated by the tuner decreases as the conductivity decreases, for high Q values, highlighting loss in the metal itself. Tuning stages that force the antenna to resonate at a frequency far form its original frequency, increase the antenna Q. For Q values high enough, the conductivity of the metal itself becomes a source of loss. Conductive loss in high-Q antennas are further investigated in the next section.

5

Table 3: Conductivity of the simulated materials

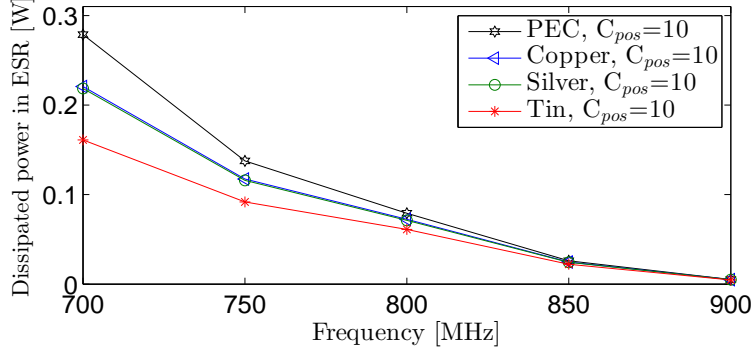|	Copper annealed	Silver	Tin
σ [S/m]	5.80 $*10^7$	6.30 $*10^7$	8.70 $*10^6$
λ_{900MHz} [m]	1.38 $*10^{-5}$	1.33 $*10^{-5}$	3.57 $*10^{-5}$
λ_{700MHz} [m]	1.57 $*10^{-5}$	1.51 $*10^{-5}$	4.05 $*10^{-5}$

Figure 7: Power dissipated in the ESR of the tuner of the high-Q antenna A2, made out of different materials.

3   Conductive loss

Narrow-band FRA's have the potential to cover a large bandwidth while exhibiting a low profile. However, the drawback of this design is its dramatically increasing Q as the resonance frequency of the antenna is tuned away from the natural resonance frequency of the design [24], i.e. the antenna is becoming electrically smaller, when operating at a lower resonance frequency than its natural resonance frequency. High-Q structures exhibit high-fields, hence a significant source of loss is the resistive loss of tuner. However, this loss alone cannot explain the measured total efficiency of FRA's [20,25]. This section investigates the existence of metal loss due to good conductors.

3.1   Theory

The radiation efficiency of an antenna is a quantity that is difficult and resource-consuming to compute, as long simulations due to high discretization of the domain are necessary for Finite-Difference Time-Domain (FDTD) methods. Therefore in most cases the radiation efficiency is measured. However the radiation efficiency can be analytically computed for simple structures - as thin dipoles - and depends on the radiation resistance (R_r) and the loss resistance (R_L). R_L is due to the conductivity of the metal and varies predominantly as the square root of frequency, as expressed below, for a uniform current distribution on a thin dipole [26]:

$$R_L = \frac{l}{p}\sqrt{\frac{\omega\mu_0}{2\sigma}},$$

where l is the length of the dipole, p is the perimeter of the wire ($p = 2\pi r$ for a wire of radius r), ω is the angular frequency, μ_0 is the permeability of free-space and σ is the conductivity. In order to demonstrate that conductive loss plays a role in high-Q antennas, the efficiency of different mock-ups, scaled with frequency, will be measured. When the frequency is doubled, the R_L is multiplied by $\sqrt{2}$ and the efficiency is multiplied by $\frac{R_r+R_L}{R_r+\sqrt{2}R_L}$, hence the efficiency drops as the frequency increases, due to conductive loss in the antenna.

3.2   Measurements

Given the frequency dependence of R_L, the existence of metal loss in narrow-band antennas is assessed using two resonance frequencies and 4 mock-ups. The antenna design, detailed in Fig. 8, is placed 2 mm above a 120 mm × 56 mm PCB. Mock-ups are shown in Fig. 9. Firstly two pure copper mock-ups are built. The
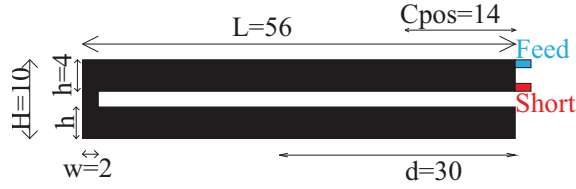
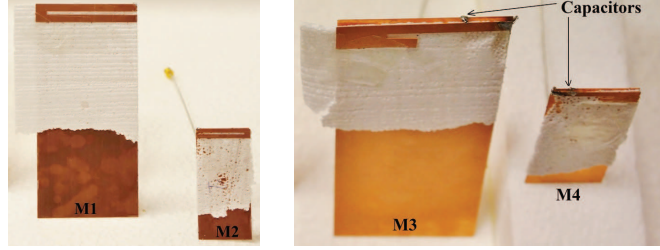Figure 8: PIFA Geometry (dimensions in mm for M1 and M3).

Figure 9: Pure copper (left) and tuned (right) mock-ups.

mock-up M1 resonates at 700 MHz and the mock-up M2 is a scaled version of M1 by a factor 1/2, thus it resonates at 1.4 GHz. M1 and M2 are made out of only copper and minimum tin is used in order to isolate the loss due to the copper alone. In particular the short of the PIFA is made out of the same copper plate as the ground to avoid soldering in high-current locations. Secondly the mock-ups M3 and M4 are built similarly to M1 and M2, except for the antenna element that is shorter (cut at the distance d) and the addition of a capacitor (at the position $Cpos$). As a result, the natural resonance frequencies of M3 and M4 are several 100 MHz higher than the ones of M1 and M2. The capacitor placed between the antenna and the ground plate tunes the mock-ups back to 700 MHz and 1.4 GHz for M3 and M4 respectively, using capacitor values of 5.1 pF and 3.0 pF.

3.3   Results

The frequency responses of the mock-ups are displayed in Fig. 10. The bandwidths of M1, M2, M3 and M4 are 10, 21, 9 and 20 MHz respectively. The difference in bandwidth between M1 and M2 corresponds to the scaling factor. The bandwidths of M3 and M4 are narrower than M1 and M2, inferring that the capacitively loaded antennas exhibit a higher Q, for the same frequency. Measured Q are plotted in Fig. 11. Bandwidth (BW) and Q relate to the Voltage-Standing-Wave Ratio (VSWR) inversely proportionally [24]:

$$Q(\omega) = \frac{2\sqrt{\beta}}{FBW_V(\omega)}, \sqrt{\beta} = \frac{s-1}{2\sqrt{s}},$$

where FBW_V is the matched VSWR fractional bandwidth and s is a specific value of the VSWR.

The loss due to the ESR of the tuner can be determined in simulations (CST) and taken out of the measured efficiency. For 1 W input power, the loss due to the ESR is summarized in Table 4. The radiation efficiency was measured in anechoic chamber and computed with 3D integration pattern. The results are summarized in Table 5.

Firstly, the loss of the mock-ups including a capacitor is significantly larger than the mock-ups only made out of pure copper. Secondly, the results show that the loss at 700 MHz is 0.8 dB and the loss at 1.4 GHz is 1.8 dB for M1 and M2, where the only source of loss is copper. These results exhibit an increasing loss

Table 4: Low-ESR capacitors

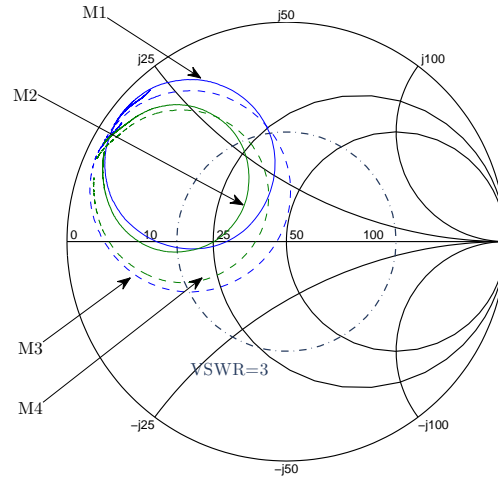| Mock-up	C [pF]	f [MHz]	ESR [Ω]	I [A]	Loss [dB]
M3	5.1	700	0.258	1.773	2.26
M4	3.0	1400	0.302	1.890	3.37

7

Figure 10: Measured frequency responses of M1 - M4.
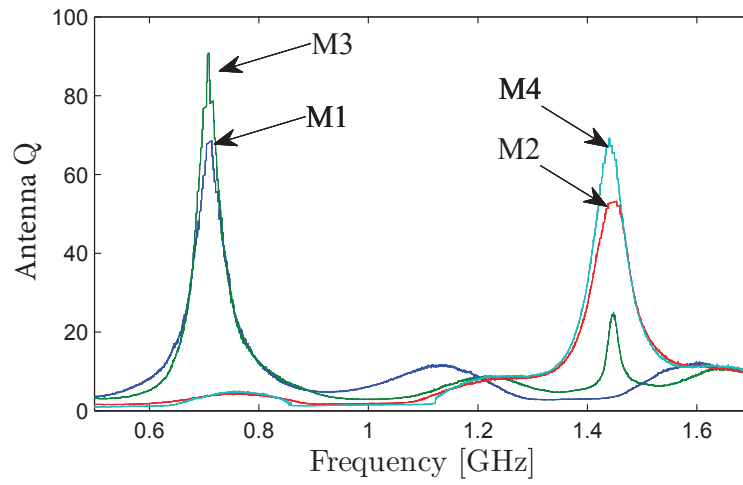
Figure 11: Measured Q of M1 - M4.

Table 5: Radiation efficiency

	M1	M3	M2	M4
f_r [MHz]	700	700	1400	1400
e_r [dB]	-0.8	-3.2	-1.8	-5.3

with frequency, confirming the existence of conductive loss in high-Q antennas. Finally, one can subtract the estimated loss due to the ESR from the measured efficiency of M3 and conclude on its conductive loss. That is to say, the measured efficiency of M3 being -3.2 dB and the simulated ESR loss being 2.26 dB, the conductive loss is estimated to be 0.9 dB. This value is in good agreement with the measured efficiency of the pure copper mock-up M1 at the same frequency, -0.8 dB. Similarly the conductive loss of M4 is estimated to be 1.9 dB ($-5.3+3.37=1.9$), which fits the measured efficiency of M2, -1.8 dB. Differences between estimations and measurements is within the chamber accuracy.

The loss of M1 and M2 is the copper loss for a mock-up exhibiting a similar Q and resonance frequency. The measured loss of M3 and M4 is consistent with the addition of copper loss (M1 and M2) and simulated ESR loss. These measurements show the existence and the significance of conductive loss in narrow-band FRA's, in addition to tuner loss.

4 Conclusion

Tunable technologies are getting mature enough to be integrated into phones. Antenna tuning can enable new front-end architectures addressing the bandwidth issue of 4G. Using narrow-band and tunable antennas allows for designs exhibiting a very low profile. However, the dramatically increasing Q of narrow-band antennas, as it is tuned, leads to thermal loss in the antenna structure itself [27]. The results presented in this paper show that the tuning loss is of two kinds: the loss due to the ESR of the tuner and the loss due to the metal conductivity. The thermal loss due to conductivity as not been an issue in typical wide-band handset antenna designs, as they exhibit a low-Q. However, novel architectures using high-Q antennas, experience a limit in achievable efficiency, due to thermal loss. If the tuner loss can be minimized with optimizing its location and future manufacturing improvements, the loss due to the metal conductivity is intrinsic to the antenna manufacturing. As the antenna is tuned towards lower frequencies, it becomes electrically smaller and higher Q, thus the conductive loss becomes significant [27]. This loss impacts directly the total efficiency of the system, therefore the feasibility of manufacturing such a design. The existence of conductive loss for narrow-band antennas is a limitation to antenna miniaturization.

References

[1] 3GPP Technical Report, "Feasibility study for Further Advancements for E-UTRA (LTE-Advanced) - Specification 36.912 - Release 11," 2012.

[2] R. F. Harrington, "Effect of Antenna Size on Gain, Bandwidth, and Efficiency," *Journal of Research of the National Bureau of Standards- D. Radio Propagation*, vol. 64D, no. 1, pp. 1–12, 1960.

[3] Y. K. Park and Y. Sung, "A Reconfigurable Antenna for Quad-Band Mobile Handset," *IEEE Transactions on Antennas and Propagation*, vol. 60, no. 6, pp. 3003–3006, 2012.

[4] H. Li, J. Xiong, Y. Yu, and S. He, "A Simple Compact Reconfigurable Slot Antenna With a Very Wide Tuning Range," *IEEE Transactions on Antennas and Propagation*, vol. 58, no. 11, pp. 3725–3728, 2010.

[5] N. Behdad and K. Sarabandi, "Dual-Band Reconfigurable Antenna With a Very Wide Tunability Range," *IEEE Transactions on Antennas and Propagation*, vol. 54, no. 2, pp. 409–416, 2006.

[6] K. Payandehjoo and R. Abhari, "Compact Multi-Band PIFAs on a Semi-Populated Mobile Handset With Tunable Isolation," *IEEE Transactions on Antennas and Propagation*, vol. 61, pp. 4814–4819, Sept. 2013.

[7] R. Valkonen, C. Luxey, J. Holopainen, C. Icheln, and P. Vainikainen, "Frequency-reconfigurable mobile terminal antenna with MEMS switches," in *Antennas and Propagation (EuCAP), 2010 Proceedings of the Fourth European Conference on*, pp. 1–5, 2010.

[8] L. Liu and R. Langley, "Electrically Small Antenna Tuning Techniques," in *Loughborough Antennas and Propagation Conference (LAPC)*, no. November, pp. 313–316, 2009.

[9] S. Caporal, D. Barrio, A. Tatomirescu, G. F. Pedersen, and A. Morris, "Novel Architecture for LTE Worldphones," *IEEE Antennas and Wireless Propagation Letters*, vol. 12, no. 1, pp. 1676–1679, 2013.

[10] J. R. De Luis, A. Morris, Q. Gu, and F. de Flaviis, "Tunable Duplexing Antenna System for Wireless Transceivers," *IEEE Transactions on Antennas and Propagation*, vol. 60, pp. 5484–5487, Nov. 2012.

[11] Y. Tsutsumi, M. Nishio, S. Obayashi, H. Shoki, T. Ikehashi, H. Yamazaki, E. Ogawa, T. Saito, T. Ohguro, and T. Morooka, "Low Profile Double Resonance Frequency Tunable Antenna Using RF MEMS Variable Capacitor for Digital Terrestrial Broadcasting Reception," in *IEEE Asian Solid-State Circuits Conference*, pp. 125–128, 2009.

[12] S. Caporal Del Barrio, A. Morris, and G. F. Pedersen, "Antenna Miniaturization with MEMS Tunable Capacitors: Techniques and Trade-Offs," *International Journal of Antennas and Propagation*, no. 709580, pp. 1–8, 2014.

[13] V. Steel and A. Morris, "Tunable RF Technology Overview," 2012.

[14] R. Cory and D. Fryklund, "Solid State RF/Microwave Switch Technology: Part 2," 2009.

[15] J. T. Aberle, "Reconfigurable Antennas for Portable Wireless Devices," *IEEE Antennas and Propagation Magazine*, vol. 45, no. 6, pp. 148–154, 2003.

[16] M. Pelosi, M. B. Knudsen, and G. F. l. Pedersen, "Multiple Antenna Systems with Inherently Decoupled Radiators," *IEEE Transactions on Antennas and Propagation*, vol. 60, no. 2, pp. 503–515, 2012.

[17] O. N. Alrabadi, A. D. Tatomirescu, M. B. Knudsen, M. Pelosi, and G. F. Pedersen, "Breaking the Transmitter-Receiver Isolation Barrier in Mobile Handsets with Spatial Duplexing," *IEEE Transactions on Antennas and Propagation*, vol. 61, no. 4, pp. 2241–2251, 2013.

[18] M. B. Knudsen, P. Bundgaard, J.-E. Mueller, G. F. Pedersen, and M. Pelosi, "Impedance Tuning of Transmitting and Receiving Antennas," *US Patent 2012/0293384 A1*, 2012.

[19] S. Caporal Del Barrio and G. Pedersen, "Antenna design exploiting duplex isolation for 4G application on handsets," *Electronics Letters*, vol. 49, pp. 1197–1198, Sept. 2013.

[20] S. Caporal, D. Barrio, M. Pelosi, G. F. Pedersen, and A. Morris, "Challenges for Frequency-Reconfigurable Antennas in Small Terminals," in *IEEE Vehicular Technology Conference (VTC Fall)*, pp. 1–5, 2012.

[21] WiSpry, "http://www.wispry.com/products-capacitors.php," 2014.

[22] Computer Simulation Technology (CST) http://www.cst.com, "CST Microwave Studio," 2012.

[23] Murata, "Chip Monolithic Ceramic Capacitors," 2012.

[24] A. D. Yaghjian and S. R. Best, "Impedance , Bandwidth , and Q of Antennas," *IEEE Transactions on Antennas and Propagation*, vol. 53, no. 4, pp. 1298–1324, 2005.

[25] S. C. D. Barrio, M. Pelosi, and G. F. Pedersen, "On the efficiency of frequency reconfigurable high-Q-antennas for 4G standards," *Electronics Letters*, vol. 48, no. 16, pp. 982– 983, 2012.

[26] C. Balanis, "2. Fundamental Parameters of Antennas," in *Antenna Theory Analysis and Design*, no. 3, ch. 2, pp. 27–132, John Wiley & Sons, 3rd ed., 2005.

[27] S. Caporal Del Barrio, G. Pedersen, P. Bahramzy, O. Jagielski, and S. Svendsen, "Thermal loss in high-Q antennas," *Electronics Letters*, vol. 50, pp. 917–919, June 2014.